Vibrational Spectroscopy 100 (2019) 48–56

Contents lists available at ScienceDirect

Vibrational Spectroscopy

journal homepage: www.elsevier.com/locate/vibspec

The influence of particle size on the intensity and reproducibility of Raman spectra of compacted samples

Diego A. Gómez, Jordi Coello, Santiago Maspoch*

Departament de Química, Facultat de Ciències, Universitat Autònoma de Barcelona, 08193, Bellaterra, Barcelona, Spain

ARTICLE INFO

Keywords:
Raman spectroscopy
Particle size
Peak intensity
Reproducibility of a raman spectrum

ABSTRACT

Given the growing interest in the application of Raman spectroscopy for quantitative purposes in solid pharmaceutical preparations, a revision of the effect of particle size on Raman spectra of compacted samples is presented. For this purpose, a set of tablets of potassium hydrogen phthalate (KHP) of different particle size were prepared. KHP was used because of its purity and stability, which allow to consider that samples will not be altered during measurements; but also because of its chemical structure (aromatic ring and carboxylic groups), that are present in many active pharmaceutical ingredients (API). The latter makes possible to consider KHP as a model pseudo-API. As KHP tablets only contain a pure compound, the mapping strategy that was considered for measuring our samples will not be affected by subsampling issues. The spectra variance can be attributed to the intrinsically reproducibility in recording the spectra (which mainly depends on the instrument set-up) and the site-to-site differences in elastic scattering properties. Two different instrumental optics have been studied: a macro-Raman system and a Raman microscope (500 μm and 50 μm laser spot size, respectively). The effect of the spectra preprocessing is also evaluated.

The overall results demonstrate raw Raman intensity increases with particle size up to a value that depends on tablet width and that the applied spectral preprocessing (baseline correction and a unit vector normalization), reduces the differences in Raman intensities due to the particle size, but does not completely eliminate it for the lower particle sizes (< 20 μm). For tablets containing particles with predefined sizes, it corrects the mapping site-to-site differences in elastic scattering.

1. Introduction

Raman spectroscopy is becoming a popular technique for the development of analytical methods applicable to several industrial fields. Among them, and probably because of the implantation of new analytical procedures in the framework of PAT (Process Analytical Technology) initiative [1], a relatively high amount of the new procedures are focused on pharmaceutical analysis, where Raman spectroscopy is being used for monitoring of different unit operations in the production chain [2–5]. When considering to analyze a solid sample using this technique, the spectrum obtained is a combination of the chemical and physical properties of the sample being measured: the first represents the main contribution to the appearance of the spectrum, which allows for example, the building of spectral libraries [6,7], or the development of quantitative methods for the determination of API(Active Pharmaceutical Ingredient) content in a solid pharmaceutical preparation [8,9]; but the latter is also important and, to some extent, its contribution is less intuitive. The main property contributing to the physical effect is particle size and, in this sense, it has been reported that the accuracy of a Raman method is affected when particle sizes of the calibration and prediction samples are different [10,11].

The theoretical relation between Raman signal and powder properties was described by Schrader et al. [12,13], as an extension of the Kubelka-Munk theory of the optical properties of crystal powders [14]. The radiation balances involved are explained by a set of differential equations, in which one of the terms corresponds to the coefficient for the elastic scattering of the sample, which is inversely proportional to the diameter of the particles. This coefficient determines, as expected, the flux of the excitation radiation, but also determines the magnitude of the flux of the inelastically scattered radiation (Raman radiation).

Two different scales regarding particle size must be considered: nano- and micro-scale. In the case of nanoparticles, as particle size reduces, subtle changes in the vibrational spectrum of the material are noticeable; these are justified in the confinement of phonons effect, and in practice presents useful information for size characterization at nanoscale [15–17].

* Corresponding author.
E-mail address: santiago.maspoch@uab.cat (S. Maspoch).

https://doi.org/10.1016/j.vibspec.2018.10.011
Received 2 October 2018; Received in revised form 26 October 2018; Accepted 26 October 2018
Available online 01 November 2018

Table 1
Experimental set-ups and main conclusions reported in previous studies regarding the influence of particle size on Raman spectra.

Ref.	Compound(s) analyzed (particle sizes)	Raman instrument	Irradiation diameter	Main findings
[18]	$Ba(NO_3)_2$, NH_4Cl, K_2CrO_4, Li_2CO_3 (105-205 μm, powders).	Backscattering FT-Raman, benchtop (1064 nm laser).	300 μm.	Raman intensities decrease as particle size increases.
[19]	$NaClO_3$, $NaBrO_3$, $K_4Fe(CN)_6 \cdot 3H_2O$, $CuSO_4 \cdot 5H_2O$, $K_3Fe(CN)_6$, $NaNO_3$ (76-605 μm, powders, $NaNO_3$ was also measured as a tablet).	Backscattering dispersive Raman (514.5 nm laser). A non-contact fiber optic probe was used, acquiring spectra in two predefined distances regarding sample position.	A) 1 mm distance = 500 μm. B) 10 mm distance = 4600 μm.	Raman intensities decrease as particle size increases. The dependence of the intensities with particle size diminishes. A maximum is observed in the intermediate fractions. A compacted sample produces less intense signals than the same sample before compaction.
[20]	Flufenamic acid, two polymorphs. (65-215 μm, powders).	Backscattering dispersive Raman (785 nm laser). Two types of fiber optic probes were used.	A) Immersion optic: 60 μm.	Each polymorph led to a different result: with one of them the variation of intensities with particle size is quite low, with the other polymorph intensities increase as particle size decreases until a maximum is reached.
			B) Non-contact sampling device (PhAT probe): 3000 μm.	Intensities do not change when the different particle size fractions are measured.
[21]	Chlorpheniramine maleate (2 % w/w) - microcrystalline cellulose (MCC) tablets (three sizes of MCC: D_{50} = 16.3, 61.7 and 178.0 μm).	Backscattering and transmission dispersive PhAT probe Raman (785 nm laser).	3000 μm.	The backscattering setting is relatively insensitive to the differences in MCC particle size, in comparison to the transmission mode.
[22]	Binary mixtures of K_2CrO_4 and $Ba(NO_3)_2$ (9 concentration levels), each compound in 8 particles sizes. (75-425 μm, powders, mixtures were measured at two compaction levels).	Backscattering dispersive Raman. Confocal microscope, 10X objective (632 nm laser). Laser beam was focused inside the sample for illuminating the whole sample surface, that was contained in a recipient with a diameter of 6.9 mm.	6900 μm.	Mixtures with the same mass fraction, but different particle size, produce spectra whose peak intensities are more different, than in the case of measuring two mixtures with different mass fraction but the same particle size. A firmly packed powder sample produces more intense peaks than a slightly compacted powder.
[23]	$CaCO_3$ (2-121 μm, powders).	Backscattering dispersive portable Raman (785 nm laser).	100 μm.	Signal increases with particle size up to the 24 μm fraction, then decreases for the larger sizes.
[24]	Ibuprofen and mannitol tablets, 5 levels of concentration, 3 compaction pressures (each compound in two sizes: ibuprofen, D_{50} = 71, 154 μm; mannitol, D_{50} = 91, 450 μm)	Transmission dispersive Raman, benchtop (785 nm laser)	4300 μm.	A Principal Component Analysis, including all the types of tablets, shows that the content and particle size of the drug substance, the particle size of the filler and, in a less extent, the compression force affect Raman spectra.
[25]	Alpha quartz (< 11 μm-250 μm, powders).	Backscattering dispersive Raman. Confocal microscope, 50X objective (488 nm laser).	2 μm.	Raman intensities increase with particle size up to a 20-30 μm fraction, then stop to increase for larger size fractions.

Considering materials in the micro-scale, which is the order of size magnitude of the compounds used for the preparation of a solid pharmaceutical form, several studies in which particle size was controlled have been described in literature, testing different inorganic salts and organic compounds and using instruments built both for transmission and/or backscattering measurements, but with some differences in the excitation source-sample arrangement. A brief summary of the experimental set-ups used, and the main conclusions reported is shown in Table 1 [18–25].

More specifically, the relation between sample particle size and the intensity of Raman signal has been mainly studied for slightly tamped powders, using instruments with different laser spot diameter (ranging from 2 μm up to more than 4000 μm). In general, the major conclusion reported has been that signal increases as particle size decreases [18–20]. However, a detailed examination of the plots of Raman intensity versus the different particle sizes tested shows that this trend is not totally fulfilled along the whole interval considered on each of these studies, being noticeable in some cases that, for the smaller sizes, intensities increase with particle size. And actually, this latter trend is what Schrader and Bergmann predict in their theoretical study. Chio et al. [25] reported an increase of the intensity starting from a fraction containing particles of less than 11 μm up to 20–30 μm, then intensities stop increasing for larger sizes. A very small irradiation spot was used in this work and, given that measurements were performed using a confocal instrument, very few particles were irradiated and a sampling deepness delimitation was possible. On the other hand, Wang et al. [19] performed Raman measurements on solid particles dispersed in different organic liquids; the experimental findings allowed them to prove that diffuse reflectance is an important mechanism in understanding the effect of particle size on Raman intensities. Nonetheless, their findings regarding the evolution of Raman intensities with particle size are opposed to the theoretically expected trend.

More recently, Kristova et al. [23] reported the effect of particle size on the fundamental vibrations of the carbonate in calcite, a mineral which internal modes have been well studied [26]. They found another change of trend in their measurements, with Raman intensities increasing with particle size up to 20 μm, and then decreasing for larger sizes. Additionally, they also found that the rate of increasing was not constant but wavenumber-dependent.

Hence, the bibliographical review of the previous experimental works shows that there are considerable differences in the main conclusions reported on them, even though the particle sizes of the fractions that were used in each case were, to some extent, overlapped.

Particle size is not an arbitrary property of the solid pharmaceutical forms currently available in the market, in fact it is an important attribute that influences some characteristics of the final product such as the dissolution rate, drug release rate for controlled release formulations, and the dosage unit content uniformity [27,28]. Tablets are the most popular of all the medicinal preparations intended for oral use [29], and Raman spectroscopy is becoming a very useful tool for the quantitative determination of API [30]. Since for this purpose, calibration samples must be prepared, it is necessary to go deeper in the understanding of the effect of particle size not only on Raman intensity, but also in the attainable precision. On the other hand, raw Raman spectra are scarcely used. It is nowadays well-known that, in order to obtain an adequate precision in a quantitative analysis, Raman spectra must be preprocessed before applying any regression model; in that sense, the standard protocol includes a baseline correction and spectral normalization [31]. The performance of this standard preprocessing procedure in the correction of the effect of particle size must be also considered.

With the aim of a better understanding of the effect of particle size in compacted tablets on Raman intensities and their reproducibility, a set of tablets of potassium hydrogen phthalate (KHP), previously grounded and sieved from < 20 μm to > 100 μm, have been prepared. KHP was chosen because it is a primary standard, what assures its chemical stability in laboratory conditions [32]. The structure of the compound also mimics a common API because of the aromatic ring of the phthalate; this functional group produces strong signals in the Raman spectra, and commonly represents the most selective analytical signal for the determination of many APIs. Results on both raw and preprocessed spectra are compared.

Raman spectra have been recorded using a FT-Raman instrument that incorporate non-contact optic sampling devices, in which the sample is placed on a software-controlled x-y-z mapping stage and illuminated via a parabolic mirror objective (macro-Raman system, 500 μm spot size), or a 10X objective (Raman microscope, 50 μm spot size). Both optics include a video camera, to visually focus the laser onto the surface and collect spectra of the measuring positions. Sets of spectra were acquired considering two acquisition modes: several successive spectra at the same measuring point (repeatability), and from different points of the measured tablets following a predefined grid (mapping). The estimation of a repeatability value is related to the best precision that can be achieved using a specific spectrometer and recording conditions, with prefixed values for spectral resolution and number of scans averaged. On the other hand, mapping is a practical solution to overcome the subsampling problem derived from the limited spot size [33] and sample heterogeneity. The differences found between the two recording procedures, in a situation where the subsampling risk is null (tablets are composed by a single compound), may be useful to measure the effect of the particle size and distribution for a given sampled area.

2. Theory

The propagation of a Raman radiation in a particulate solid sample was studied by Schraeder and Bergmann, as an extension of the Kubelka-Munk theory for diffuse reflectance radiation. From the definition of an elastic (r) and an inelastic (s) scattering coefficients, and after solving the radiative transfer equations, one of their findings was that the intensity of the backscattered Raman radiation could be described by the following equation

$$\overleftarrow{\varnothing_R} = \overrightarrow{\varnothing_0}\frac{s\,k}{a}\left\{\frac{k\,sinh^2\,kd + (a+r)\sinh kd\cosh kd - krd}{[(a+r)\sinh kd + \cosh kd]^2}\right\} \quad (1)$$

Where $\overleftarrow{\varnothing_R}$ is the Raman radiation emerging from the irradiated face, $\overrightarrow{\varnothing_0}$ is the irradiation flux, and, s and r, are respectively, the linear Napierian absorption, elastic scattering and Raman scattering coefficients. k is a parameter related to a and r.

By considering that the elastic coefficient is proportional to the reciprocal of the particle diameter, and after assigning values to a, s and k, the main conclusions Schraeder and Bergmann obtained were that backscattered Raman intensity should:

i) Increase with particle diameter
ii) Increase with sample thickness but should arrive to a plateau after a certain penetration into the sample. The depth of this penetration increases with particle size, and for particles of low and medium diameter (10–100 μm) should be in the range of 1–4 mm

As pointed out by McCreery [34], for a FT spectrometer, the signal magnitude for a given Raman shift value is proportional to the photons observed for that Raman shift only, while the noise has contributions from all Raman shift values. This leads to the condition that the expected standard deviation should be constant at all wavenumbers, and function of the instrument characteristics and recording set-up. This is true if spectra are measured exactly at the same point of the sample, but if spectra are recorded at different positions on tablet surface, the differences in the elastic scattering must also be considered. The elastic scattering coefficient mainly depends on particles size distribution, but also on differences in refraction indexes, surfaces orientation, etc.

Another contribution that will affect the reproducibility of spectra acquisition is the slight differences in focusing because tablets are not always placed in a perfect horizontal position.

Consequently, the expected variance (s^2) in mapping measurements can be described as:

$$s^2 = s_a^2 + s_s^2 + s_f^2 + s_m^2 \quad (2)$$

Where s_a^2 is the intrinsic analytical variance when recording a spectrum (function of the instrumental set-up: spectral resolution, number of scans averaged); s_s^2 is the variance produced by the differences in scattering between different positions of the same sample; s_f^2 is the variance due to focus variability; and s_m^2 accounts for the differences in composition of the sampled volume when analyzing complex mixtures. Since s_s^2 and s_f^2 cannot be differentiated separately, both terms can be joined and expressed simply as 'scattering effect'. In the case of recording Raman spectra of a sample containing a single compound s_m^2 can be neglected and (2) simplifies to:

$$s^2 = s_a^2 + s_s^2 \quad (3)$$

From a practical point of view, for a given instrumental set-up, s_a can be estimated recording the spectra at the same measuring position. Along the text, this recording mode will be referred as a repeatability measurement.

3. Materials and methods

3.1. Preparation of tablets

Potassium hydrogen phthalate (KHP) (Fluka, Switzerland) was initially dried at 105 °C, and then grounded by hand with a mortar and pestle. Subsequently, six fractions of different particle diameter were obtained by dry sieving using a RP.15 laboratory sieve shaker (CISA, Barcelona, Spain). The nominal aperture of the available sieves (CISA, Barcelona, Spain) was 20 μm, 25 μm, 50 μm, 75 μm and 100 μm (fractions will be denoted in figures as: < 20 μm = 10 μm, 20–25 μm = 22.5 μm, 25–50 μm = 37.5 μm, 50–75 μm = 62.5 μm, 75–100 μm = 87.5 μm, 100–150 μm = 125 μm). The powder from each fraction was used to prepare a compacted sample in the form of a disc using a Perkin Elmer 15.001 hydraulic tablet press (Waltham, MA, USA): 300 mg of each fraction was used for the preparation of the tablets; the resulting disks have a diameter of 13.4 mm and a thickness of 1.4 mm for all the fractions except for the > 100 μm fraction, which thickness was 1.5 mm. The compaction pressure was 140 MPa for all the samples.

3.2. Instruments and software

Raman spectra were acquired using two different instruments: a conventional macro-Raman system (Brüker MultiRam spectrometer, Billerica, MA, USA) and a Raman microscope equipped with a 10X objective (RamanScope III, Billerica, MA, USA); both instruments use a Nd:YAG laser as excitation source (1064 nm) with a spot size of 500 μm and 50 μm respectively, and a liquid N_2 cooled Ge diode detector. A software-controlled x-y-z stage is available in both instruments, which allows controlled and reproducible mapping measurements. The Raman microscope was also used as an optical microscope to visually confirm the fractions obtained after sieving. Opus 7.1 was used for system control and to export data. All the spectra were preprocessed using Unscrambler 10.3 (Trondheim, Norway).

3.3. Spectral acquisition

The spectra were recorded in two different ways: 10 measurements at the same point (repeatability) and 10 measurements at different points of the tablet surface (mapping). One of the fractions was also measured before compaction. Each spectrum was acquired from 50 to 3600 cm^{-1} with a spectral resolution of 1 cm^{-1}, and after averaging 32 scans. The laser power was set at 400 mW. Previously it was confirmed that this relatively high laser power did not have any effect on KHP stability. For mapping acquisition, the system was optically focused on a central point of the tablet, and a grid of 10 point was recorded. To avoid tablet displacements, they were fixed on an aluminum disk fitted on the x-y-z stage.

3.4. Spectral preprocessing

Baseline corrections (baseline offset and slope of the spectrum, abbreviated BLC), and a normalization to a unit vector length (UNorm) were applied to study the effect of these pretreatments on the intensities and reproducibility of the peaks, in comparison to the raw spectra. The experimental findings related to the Raman intensities are discussed considering three wavenumbers (band assignments according Ref. [35]): 1675 cm^{-1} (C═O stretching), 1601 cm^{-1} (CC_t stretching) and 1039 cm^{-1} (CH bending in plane).

4. Results and discussion

4.1. Effect of compacting powder

Since most of the previous published studies have been performed on powders, initially, a set of spectra were acquired on the 20–25 μm particle size fraction without compaction: the powder was only gently flattened using a laboratory spatula over the measuring platform in the sample compartment of the spectrometer, employing the proper amount of sample to obtain approximately the same thickness that in compacted samples, and 10 spectra were recorded as mapping on the macro-Raman system.

The average of 10 spectra for the loosely packed and compacted sample are overlaid in Fig. 1. As can be seen, the measurement of a compacted sample results in a significantly more intense spectrum (Fig. 1A). In this first comparison, only the compaction level introduces a difference between samples, as both possess the same particle size. Hence, the difference between spectra reflects the difference in two

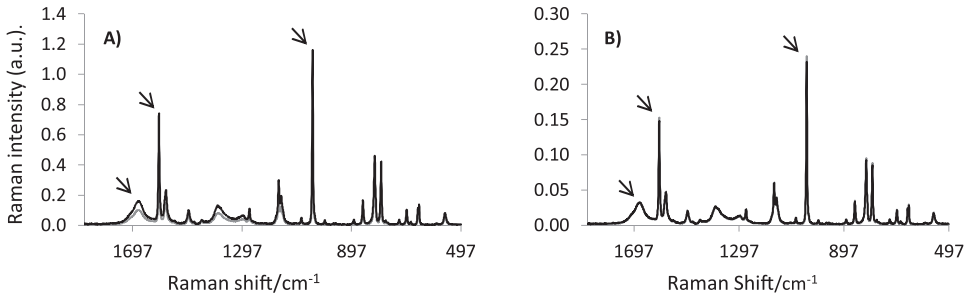

Fig. 1. Overlapped Raman spectra of the loosely packed (grey line) and compacted (black line) for the 22.5 μm fraction. A) Raw spectra, B) Spectra after baseline corrections and unit vector normalization. The arrows denote the wavenumbers selected for the intensity measurements (1674, 1601,1039 cm^{-1}).

physical characteristics of the measured sample: the packing degree between particles, and a resulting porosity. A high-power laser is irradiated on the sample, and in each case, there is a number of scattering molecules that will produce a Raman signal. As the intensities are stronger in the compacted sample, this suggests that a higher number of molecules are involved in the resulting response. This can be attributed to an increase in the density of the sampled material and a decrease of the elastic scattering coefficient, in perfect concordance with what it is expected from Kubelka-Munk theory, and has been previously reported for Near Infrared (NIR) reflectance measurements [36]. Wang et al. [19] reported a similar comparison using $NaNO_3$, however in their experiments a compacted sample produced less intense signals than the corresponding powder; they mentioned that this result was counter-intuitive, but consistent with the other results found using the same optical system, formed by parallel optical fibers. Chen et al. [22] also presented the powder/compacted sample spectra for a K_2CrO_4/Ba $(NO_3)_2$ mixture, in this case a compacted sample resulted in more intense peaks than those of a loosely packed sample. A confocal Raman microscope was used in this study.

In summary, it is clear that instrument optics determines the experimental findings and must be taken into account when the results from previous studies are interpreted. This is made more evident in Table 1, where the results reported of the effect of particle size on Raman intensity have been summarized, showing different conclusions depending on the experimental set-ups used in each case.

After applying the spectral preprocessing (Fig. 1B), it is no longer possible to distinguish the samples by their compaction degree. Table 2 presents the intensity values for the wavenumbers selected, and the corresponding standard deviation for the 10 positions measured. The absolute standard deviation values for the measurements on the compacted and loosely packed samples are of the same order (variances are homogeneous according to an F-test). However, and because of the different signal intensity, the percent relative standard deviation (RSD %) of the measurements performed on the tablet (2.5–3 %), is almost half of the RSD% value obtained from the powder sample (5%) when raw spectra are compared. After spectral preprocessing, the RSD% is practically the same for the compacted and powdered sample, and it is reduced by a factor of 4–5, yielding RSD% values in the range of 0.3–1.6 %.

4.2. Evolution of Raman intensities with particle size in compacted samples

Powders were compacted at 140 MPa, a standard compaction pressure in pharmaceutical tablet manufacturing. In a previous study, it was found that considering tablet compaction pressures ranging from 140 to 700 MPa are not distinguish in the acquired Raman spectra after applying a spectra normalization [8].

In the next sections, the evolution of Raman peak intensities with particle size will be explained considering the strategy in which spectra were acquired; the results of the measurements in the same position (repeatability) will be presented first, and then the results found in mapping mode. Thereafter, a joint discussion of the repeatability and mapping measurements will be presented.

4.2.1. Repeatability results

Fig. 2 depicts the results found. As can be seen, the trend is very similar for both optical systems: an increment in signal intensity with particle size is clearly observed in raw spectra for the fractions of smaller size, up to a value around 40 μm, from which the intensity values stabilize and are independent of particle size (Fig. 2A and C). The evolution of Raman intensities for the smaller fractions, agrees with what would be expected for a system controlled by the diffuse reflectance effect: Raman signal increases when particle size increases. The repeatability is quite good, with RSD% values (n = 10) in the range of 0.2–1 %, and 1–5 %, for the macro-Raman system and Raman microscope respectively, producing error bars that are hardly detected at the graphical scale of the figure.

The stabilization of the Raman intensity from a determined particle size can be understood if we consider the depth (volume) of sample from which the Raman radiation collected in backscattering mode comes from. In their theoretical approach, assuming specific values for a and k (Eq. 1), Schrader and Bergmann found that the intensity of the backscattered Raman radiation should arrive to a plateau at a sample depth of around 1.5 mm for a particle size of 10 μm and 4 mm for 100 μm. This result is in a good agreement with the conclusions reported by Matousek and Parker [37], who found, from a simulation model where elastic and inelastic radiations propagate in the medium in random-walk-like fashion within a three dimensional space, that for a particle size of 10 μm, the 88% of the backscattered Raman radiation was produced in the first millimeter of sample depth, and less than 3% after 1.5 mm.

Going back to our results, Fig. 3 depicts the intensity recorded at 1601 cm^{-1} for KHP tablets containing particles corresponding to the 22.5 and 125 μm fractions, as a function of tablet thickness. In a good agreement with the theoretical findings described above, the intensity increases with the particle size, arrives to a plateau after a defined sample thickness, and that this stabilization thickness increases with particle size (1.1–1.2 mm for 22.5 μm fraction and 1.4–1.5 mm for 125 μm). Despite that our results show a lower increment than the theoretical prediction in the variation of penetration with particle size, the relevant fact is that the trend predicted by the theory is experimentally corroborated.

It must be kept in mind that the tablets prepared for the experimental design shown in Fig. 2 had a thickness around 1.4–1.5 mm; in this manner, once arrived at the particle size for which this is the maximum depth of penetration, it should be expected that the intensity would remain constant, even for increasing particle sizes. The latter is what it is actually observed. And finally, it should be pointed out that even for a relatively large particle size (125 μm), the sample depth from which the Raman spectrum is acquired is relatively small, emphasizing the fact that, using a backscattering Raman spectrometer, the acquired spectra mainly possess information from only the surface irradiated.

After the spectral preprocessing (Fig. 2B and D), the effect of particle size on peak intensities is considerably reduced, however an ANOVA test ($\alpha = 0.05$) shows that for the 1039 cm^{-1} and 1601 cm^{-1} peaks, there are still significant differences between fractions. These differences arise from the fraction of smaller particle size (< 20 μm) which intensity is slight but statistically different of the intensity for other particle sizes.

Table 2
Effect of compaction on Raman intensities for the sample of 20–25 μm measured by mapping (n = 10) in the macro-Raman system. Intensity, standard deviation in brackets and RSD%, before and after spectral preprocessing.

	Raw data		Preprocessed	
Wavenumber/cm^{-1}	Powder	Tablet	Powder	Tablet
1675	0.102 (0.005) 4.9 %	0.163 (0.005) 3.1 %	0.0320 (0.0005) 1.6 %	0.0322 (0.0003) 0.9 %
1601	0.487 (0.022) 4.5 %	0.776 (0.020) 2.6 %	0.1532 (0.0005) 0.3 %	0.1529 (0.0008) 0.5 %
1039	0.764 (0.037) 4.8 %	1.220 (0.032) 2.6 %	0.2402 (0.0015) 0.6 %	0.2406 (0.0015) 0.6 %

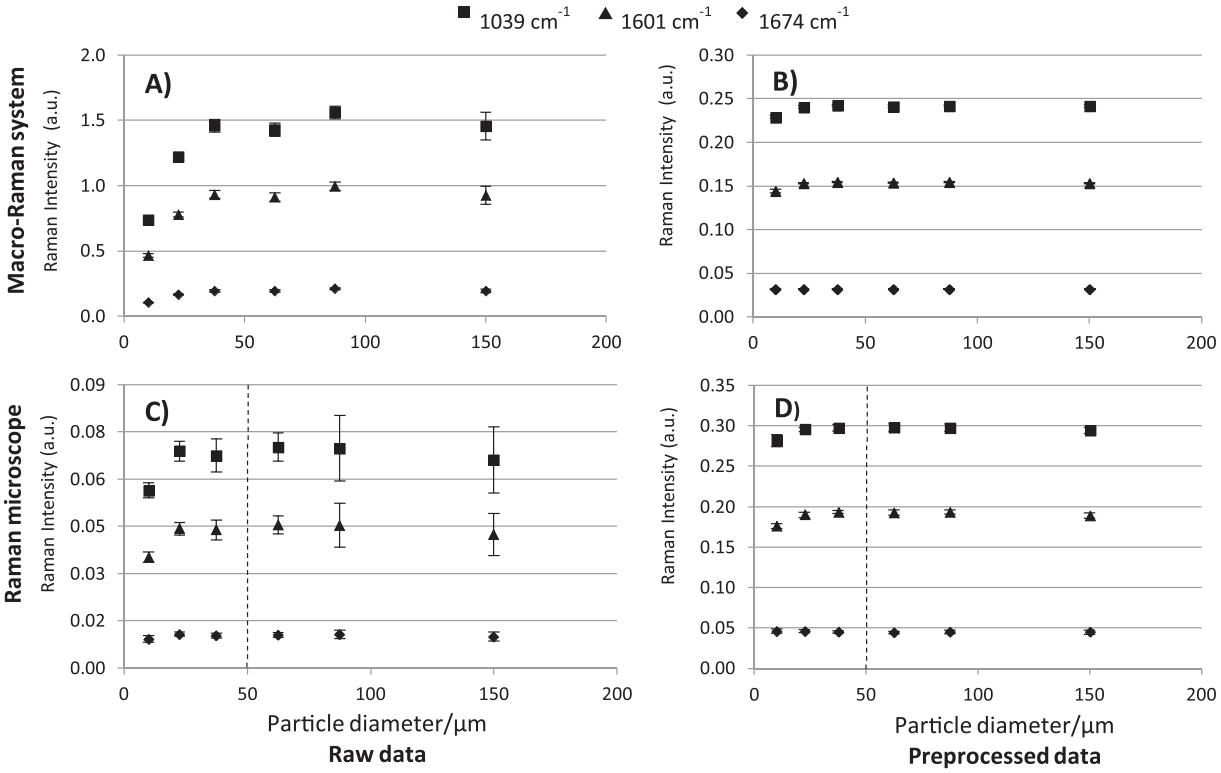

Fig. 2. Evolution of peak Raman intensity and standard deviation of repeatability measurements (n = 10 spectra) of compacted KHP tablets with particle size. Macro-Raman system: A) raw spectra; B) after spectral preprocessing. Raman microscope: C) raw spectra; D) after spectral preprocessing. In C) and D) the vertical line indicates the laser spot diameter.

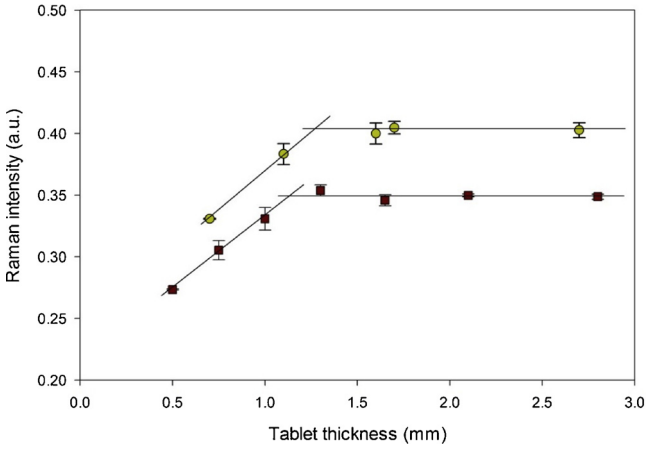

Fig. 3. Average and standard deviation of Raman intensity at 1601 cm^{-1} measured on KHP tablets of different thickness using the macro-Raman system. Particle size 22.5 µm (red squares) and 125 µm (yellow dots). Spectra acquired at a laser power of 400 mW, averaging 128 scans, 6 measurements in different positions of the same tablet. Lines drawn only to visualize the trends.

4.2.2. Mapping results

Fig. 4 shows the average peak height and its standard deviation versus particle size, when recording the spectra by mapping, using a grid of 10 points. The same trend described above is found: an increase in Raman intensities from < 20 µm up to around 50 µm, is again observed.

As expected, given that tablets are solely constituted by a pure component, the average intensity for each particle size is the same than in repeatability measurements. It is interesting to note that the magnitude of the standard deviation increases for the larger fractions. Since the object being measured is a homogeneous sample, this fact cannot be attributed to the well-known subsampling problem of Raman spectroscopy, and must be interpreted in terms of the differences in elastic light scattering (Eq. 3). A similar trend (variance increases with particle size) is widely known for NIR spectroscopy [38]. Even though the effect is lower in Raman spectroscopy than in NIR, it must be highlighted that in both cases the same trend is found. Moreover, the different relations between the laser diameter (500 µm), and the size of the particles being measured, must be kept in mind; as a result the major amplitude of the error bars for the larger fractions (Fig. 4A), can be justified in the more significant impact of the individual arrangement of the particles in comparison when the total number of particles irradiated diminished.

The relative higher increase of the standard deviation with particle size when using a microscope (Fig. 4C) can be attributed to the smaller sampled area. In this case, the scattering effect is enhanced because of the smaller number of particles being irradiated. Having a laser spot size of 50 µm, it seems that when the diameter of particles exceeds this value, the specific arrangement of the individual particles will significantly determine the intensity of the resulting spectrum acquired in each of the sampling positions.

The spectral preprocessing minimizes the particle size-dependent variations in Raman intensities (Fig. 4B and D), however, an ANOVA test shows again that there are still significant differences for the 1039 cm^{-1} and 1601 cm^{-1} bands, similarly to the previously discussed observation for repeatability measurements: the intensity for the smaller fraction (< 20 µm) is significantly different from the other sizes.

4.3. Comparison between mapping and repeatability measurements

For a better visualization of the different trend in peak reproducibility, the evolution of standard deviations and the corresponding RSD % for the Raman intensity at 1601 cm^{-1} before and after the spectral preprocessing is depicted in Fig. 5 as a function of the particle size. It is clear that, while there is a difference between mapping and

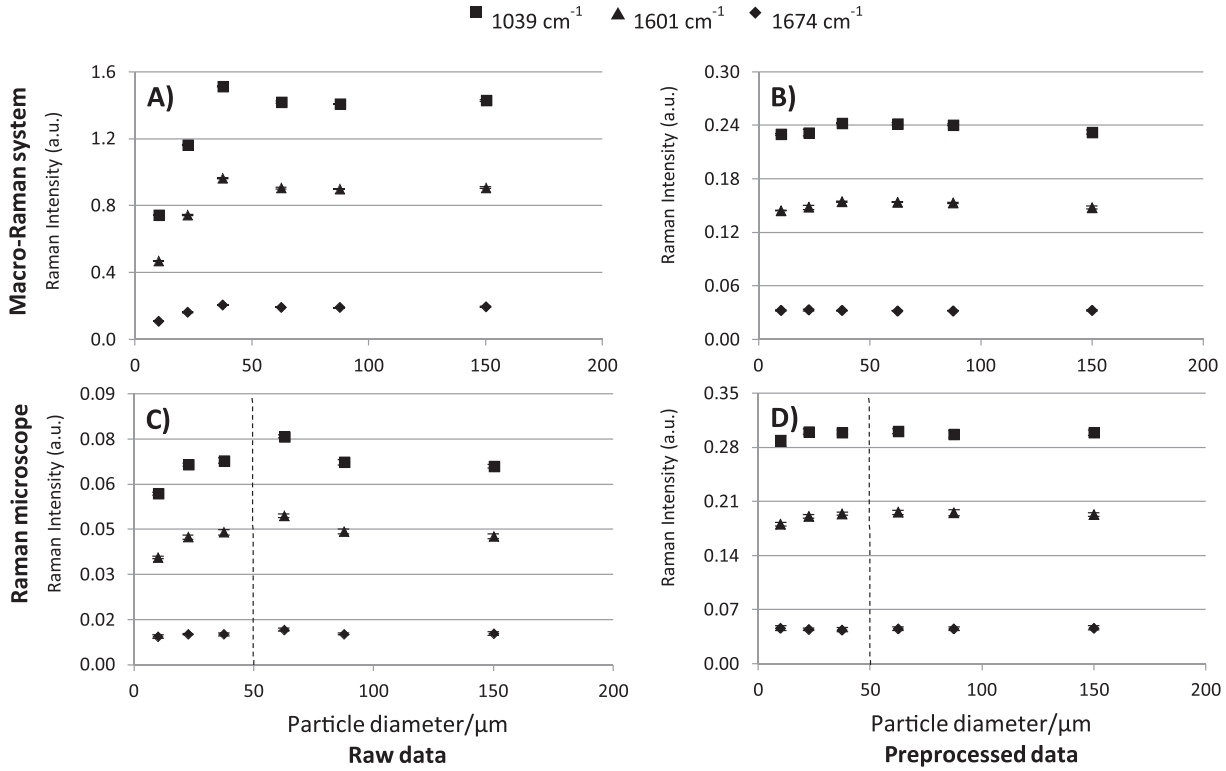

Fig. 4. Evolution of the average peak Raman intensity and standard deviation of mapping measurement (n = 10 spectra) of compacted KHP tablets with particle size. Macro-Raman system: A) raw spectra; B) after spectral preprocessing. Raman microscope: C) raw spectra; D) after spectral preprocessing. In C) and D) the vertical line indicates the laser spot diameter.

repeatability measurements when considering raw spectra, this difference disappears after the spectral preprocessing. An F test (one-tailed, $\alpha = 0.05$) confirms that, for raw spectra, variances of mapping measurements are significantly higher than the variances of repeatability measurements. After the spectral preprocessing, variances become homogeneous. This fact can be interpreted in terms described in

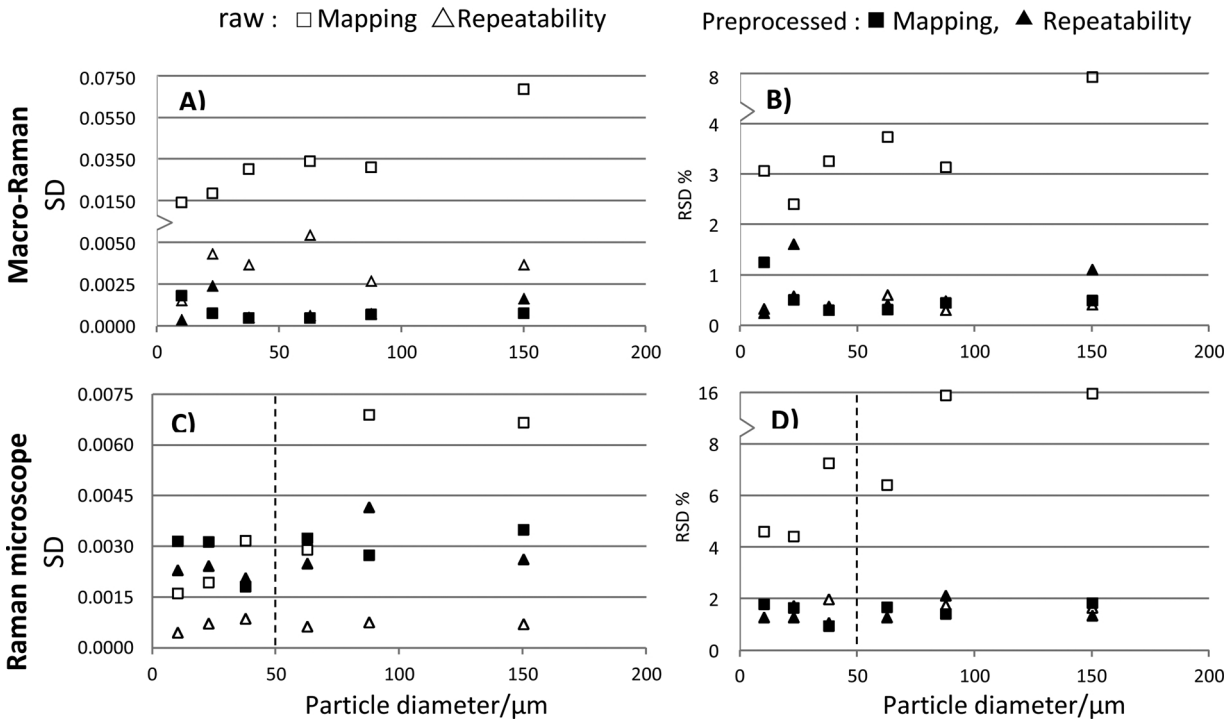

Fig. 5. Evolution of standard deviation (SD) and percent relative standard deviation (RSD %) of Raman intensity at 1601 cm^{-1} with particle size, both for mapping and repeatability measurements. Macro-Raman system: A) SD, B) RSD %. Raman microscope: C) SD, D) RSD %. In C) and D) the vertical line indicates the laser spot size.

Eq. 3. The variance recorded in mapping mode is the combination of two sources of variability, the intrinsic repeatability and the differences in elastic scattering between different points of the tablet surface. The fact that the relative standard deviation (RSD%) after spectral preprocessing overlap with the values obtained in repeatability conditions (Fig. 5B and D), strongly suggest that the elastic scattering variability is practically removed after a normalization step.

5. Conclusion

When irradiating a particulate sample to acquire a Raman spectrum, the excitation flux moves throw the sample by multiple elastic processes of scattering, and a small fraction of the scattered photons suffer Raman scattering. Thereafter, the Raman scattered radiation also travels inside the sample through a diffuse reflectance scattering mechanism. This mechanism is the qualitative basis of the Schrader and Bergmann theoretical approach [19,20]. The effect of particle size in the diffuse reflectance mechanism has been studied and demonstrated in a large number of works in NIR Spectroscopy [39,40]. From a qualitative point of view, Raman intensity should be affected by particle size in a comparable way than in NIR. Hence, an increment of intensity with particle size should be expected.

Our results are in a good agreement with this assumption. Raman intensities are lower for the smaller particle size fractions and increase up to a size of approximately 40–50 μm. For larger particle sizes intensity arrives to a plateau. An intuitive explanation to the intensity stabilization could be that the amount of sample that produces a Raman scattering able to leave the sample in a backscattering mode becomes constant. In fact, as predicted by theory [19], calculated by simulations [37] and experimentally verified in this work, Raman spectra recorded in backscattering mode, comes from a thin sample layer which thickness depends on the particle size. In this work, the laboratory prepared tablets had a thickness of 1.4–1.5 mm. This value is approximately the estimated penetration depth for compacted particles with a diameter in the range 40–50 μm. Consequently, the Raman intensity becomes constant for higher particle sizes, just because the whole tablet has been sampled. Taking into account the particle sizes used in pharmaceutical tablets, a penetration depth of 1–1.5 mm has to be expected, and actually this should be considered in the design of the calibration sample set, as well as in the interpretation of the quantitative results obtained.

The spectral preprocessing used in this work considerably reduces the effect of particle size on signal intensities, but it must be emphasized that a small but significant difference has been still found for the smallest particle size (< 20 μm). Measurements reproducibility is also a function of particle size. RSD% in repeatability conditions (i.e. same position in tablet) represents the best possible value attainable and it is a function of the spectrometer set up (mainly spectral resolution and number of scans averaged). RSD% of values obtained in mapping mode are significantly higher than those obtained when measuring in the same position, but in this case the spectral preprocessing practically eliminates the elastic scattering variations, producing mapping variances comparable to those obtained in repeatability conditions. Similar trends are found both for the macro Raman system and the microscope, however for the latter, the lower amount of particles sampled, and the lower magnitude of the acquired signals, produce higher RSD% values.

Acknowledgements

This research was funded by MINECO (Spain) through the project CTQ 2016-79696-P (AEI/FEDER, EU). Raman spectrophotometer was partly acquired with the financial support of AQU (Agencia per a la Qualitat del Sistema Universitari de Catalunya) through the project 2009 SGR 1470.

References

[1] U.S.D. Of H. And H.S. Fda, Guidance for Industry PAT — a Framework for Innovative Pharmaceutical Development, Manufacuring, and Quality Assurance, (2004), p. 16 http://www.fda.gov/downloads/Drugs/GuidanceComplianceRegulatoryInformation/Guidances/ucm070305.pdf.
[2] J. Kim, J. Noh, H. Chung, Y.-A. Woo, M.S. Kemper, Y. Lee, Direct, non-destructive quantitative measurement of an active pharmaceutical ingredient in an intact capsule formulation using Raman spectroscopy, Anal. Chim. Acta 598 (2007) 280–285, https://doi.org/10.1016/j.aca.2007.07.049.
[3] T. Vankeirsbilck, A. Vercauteren, W. Baeyens, G. Van der Weken, F. Verpoort, G. Vergote, J.P. Remon, Applications of Raman spectroscopy in pharmaceutical analysis, Trends Analyt. Chem. 21 (2002) 869–877, https://doi.org/10.1016/S0165-9936(02)01208-6.
[4] S.C. Pinzaru, I. Pavel, N. Leopold, W. Kiefer, Identification and characterization of pharmaceuticals using Raman and surface-enhanced Raman scattering, J. Raman Spectrosc. 35 (2004) 338–346, https://doi.org/10.1002/jrs.1153.
[5] G. Févotte, In situ raman spectroscopy for in-line control of pharmaceutical crystallization and solids elaboration processes: a review, Chem. Eng. Res. Des. 85 (2007) 906–920, https://doi.org/10.1205/cherd06229.
[6] J.D. Rodriguez, B.J. Westenberger, L.F. Buhse, J.F. Kauffman, Standardization of Raman spectra for transfer of spectral libraries across different instruments, Analyst 136 (2011) 4232, https://doi.org/10.1039/c1an15636e.
[7] C.M. Gryniewicz-Ruzicka, J.D. Rodriguez, S. Arzhantsev, L.F. Buhse, J.F. Kauffman, Libraries, classifiers, and quantifiers: a comparison of chemometric methods for the analysis of Raman spectra of contaminated pharmaceutical materials, J. Pharm. Biomed. Anal. 61 (2012) 191–198, https://doi.org/10.1016/j.jpba.2011.12.002.
[8] J. Arruabarrena, J. Coello, S. Maspoch, Raman spectroscopy as a complementary tool to assess the content uniformity of dosage units in break-scored warfarin tablets, Int. J. Pharm. 465 (2014) 299–305, https://doi.org/10.1016/j.ijpharm.2014.01.027.
[9] D.A. Gómez, J. Coello, S. Maspoch, Raman spectroscopy for the analytical quality control of low-dose break-scored tablets, J. Pharm. Biomed. Anal. 124 (2016) 207–215, https://doi.org/10.1016/j.jpba.2016.02.055.
[10] T.R. De Beer, W.R. Baeyens, Y.V. Heyden, J.P. Remon, C. Vervaet, F. Verpoort, Influence of particle size on the quantitative determination of salicylic acid in a pharmaceutical ointment using FT-Raman spectroscopy, Eur. J. Pharm. Sci. 30 (2007) 229–235, https://doi.org/10.1016/j.ejps.2006.11.009.
[11] N. Townshend, A. Nordon, D. Littlejohn, J. Andrews, P. Dallin, Effect of particle properties of powders on the generation and transmission of Raman scattering, Anal. Chem. 84 (2012) 4665–4670, https://doi.org/10.1021/ac203446g.
[12] B. Schrader, G. Bergmann, Die Intensität des Ramanspektrums polykristalliner Substanzen, Fresenius' Zeitschrift Für Anal. Chemie. 225 (1967) 230–247.
[13] B. Schrader, A. Hoffmann, S. Keller, Near Infrared Fourier transform Raman spectroscopy, facing absorption and background.pDf, Spectrochim. Acta Part A Mol. Spectrosc. 47 (1991) 1135–1148.
[14] P. Kubelka, F. Munk, Ein Beitrag zur Optik der Farbanstriche, Zeit. Für Tekn. Phys. 12 (1931) 593–601.
[15] S. Singh, H. Zeng, C. Guo, W. Cai (Eds.), Nanomaterials: Processing and Characterization With Lasers, Wiley-YCH, 2012.
[16] A.K. Arora, M. Rajalakshmi, T.R. Ravindran, V. Sivasubramanian, Raman spectroscopy of optical phonon confinement in nanostructured materials, J. Raman Spectrosc. 38 (2007) 604–617, https://doi.org/10.1002/jrs.1684.
[17] S. Osswald, V.N. Mochalin, M. Havel, G. Yushin, Y. Gogotsi, Phonon confinement effects in the Raman spectrum of nanodiamond, Phys. Rev. B 80 (2009) 075419, , https://doi.org/10.1103/PhysRevB.80.075419.
[18] M.V. Pellow-Jarman, P.J. Hendra, R.J. Lehnert, The dependence of Raman signal intensity on particle size for crystal powders, Vib. Spectrosc. 12 (1996) 257–261, https://doi.org/10.1016/0924-2031(96)00023-9.
[19] H. Wang, C.K. Mann, T.J. Vickers, Effect of powder properties on the intensity of raman scattering by crystalline solids, Appl. Spectrosc. 56 (2002) 1538–1544.
[20] Y. Hu, H. Wikström, S.R. Byrn, L.S. Taylor, Analysis of the effect of particle size on polymorphic quantitation by raman spectroscopy, Appl. Spectrosc. 60 (2006) 977–984.
[21] N. Townshend, A. Nordon, D. Littlejohn, M. Myrick, J. Andrews, P. Dallin, Comparison of the determination of a low-concentration active ingredient in pharmaceutical tablets by backscatter and transmission raman spectrometry, Anal. Chem. 84 (2012) 4671–4676, https://doi.org/10.1021/ac203447k.
[22] Z.P. Chen, L.M. Li, J.W. Jin, A. Nordon, D. Littlejohn, J. Yang, J. Zhang, R.Q. Yu, Quantitative analysis of powder mixtures by raman spectrometry: The influence of particle size and its correction, Anal. Chem. 84 (2012) 4088–4094, https://doi.org/10.1021/ac300189p.
[23] P. Kristova, L.J. Hopkinson, K.J. Rutt, The effect of the particle size on the fundamental vibrations of the [CO_3^{2-}] anion in calcite, J. Phys. Chem. A 119 (2015) 4891–4897, https://doi.org/10.1021/acs.jpca.5b02942.
[24] A. Sparén, M. Hartman, M. Fransson, J. Johansson, O. Svensson, Matrix effects in quantitative assessment of pharmaceutical tablets using transmission raman and near-infrared (NIR) spectroscopy, Appl. Spectrosc. 69 (2015) 580–589, https://doi.org/10.1366/14-07645.
[25] C.H. Chio, S.K. Sharma, P.G. Lucey, D.W. Muenow, Effects of particle size and laser-induced heating on the raman spectra of alpha quartz grains, Appl. Spectrosc. 57 (2003) 774–783, https://doi.org/10.1366/000370203322102852.
[26] M. De La Pierre, C. Carteret, L. Maschio, E. André, R. Orlando, R. Dovesi, The Raman spectrum of CaCO3 polymorphs calcite and aragonite: a combined experimental and computational study, J. Chem. Phys. 140 (2014) 164509, , https://doi.

org/10.1063/1.4871900.
[27] B.Y. Shekunov, P. Chattopadhyay, H.H.Y. Tong, A.H.L. Chow, Particle size analysis in pharmaceutics: principles, methods and applications, Pharm. Res. 24 (2007) 203–227, https://doi.org/10.1007/s11095-006-9146-7.
[28] B.R. Rohrs, G.E. Amidon, R.H. Meury, P.J. Secreast, H.M. King, C.J. Skoug, Particle size limits to meet USP content uniformity criteria for tablets and capsules, J. Pharm. Sci. 95 (2006) 1049–1059, https://doi.org/10.1002/jps.
[29] Z.I. Hanan, J.M. Durgin, Pharmacy Practice for Technicians, 5th ed., Cencage Learning, New York, 2015.
[30] S. Šašić (Ed.), Pharmaceutical Applications of Raman Spectroscopy, John Wiley & Sons, Inc., 2008.
[31] S.J. Fraser, K.C. Gordon, Raman spectroscopy in the study of pharmaceuticals: the problems and solutions to sub-sampling and data analysis, Riv. Eur. Sci. Med. Farmacol. 19 (2014) 3–8.
[32] M. Csuros, Environmental Sampling and Analysis. Lab Manual, CRC Press, 1997.
[33] S.E.J. Bell, J.R. Beattie, J.J. McGarvey, K.L. Peters, N.M.S. Sirimu, S.J. Speers, Development of sampling methods for Raman analysis of solid dosage forms of therapeutic and illicit drugs, J. Raman Spectrosc. 35 (2004) 409–417, https://doi.org/10.1002/jrs.1160.
[34] R.L. McCreery, Raman Spectroscopy for Chemical Analysis, John Wiley & Sons, Inc., 2000.
[35] B. Orel, D. Hadži, F. Cabassi, Infrared and Raman Spectra of potassium hydrogen phthalate, Spectrochim. Acta Part A Mol. Spectrosc. 31 (1975) 169–182.
[36] J. Arruabarrena, J. Coello, S. Maspoch, Enhancing sensitivity and precision on NIR reflectance determination of an API at low concentration: application to an hormonal preparation, J. Pharm. Biomed. Anal. 60 (2012) 59–64, https://doi.org/10.1016/J.JPBA.2011.10.026.
[37] P. Matousek, A.W. Parker, Bulk raman analysis of pharmaceutical tablets, Appl. Spectrosc. 60 (2006) 1353–1357, https://doi.org/10.1366/000370206779321463.
[38] M. Blanco, J. Coello, H. Iturriaga, S. Maspoch, F. Gonzalez, R. Pous, Effect of the sample cell module and particle size on the NIRS determination of piracetam, Near Infrared Spectroscopy: Bridging the Gap Between Data Analysis and NIR Applications, Ellis Horwood, Chichester, 1992.
[39] D.J. Dahm, K.D. Dahm, Interpreting Diffuse Reflectance and Transmittance. A Theoretical Introduction to Absorption Spectroscopy of Scattering Materials, NIR Publications, 2007.
[40] P. Williams, K. Norris (Eds.), Near-Infrared Technology in Agricultural and Food Industries, Am Assoc. Cereal Chemists, St Paul, Minnesota, 1987.